Journal of Hydrology 564 (2018) 836–845

Contents lists available at ScienceDirect

Journal of Hydrology

journal homepage: www.elsevier.com/locate/jhydrol

Research papers

Estimating groundwater discharge to a lowland alluvial stream using methods at point-, reach-, and catchment-scale

Rasmus Rumph Frederiksen*, Steen Christensen, Keld Rømer Rasmussen

Department of Geoscience, Aarhus University, Høegh-Guldbergs Gade 2, 8000 Aarhus C, Denmark

ARTICLE INFO

This manuscript was handled by Marco borga, Editor-in-Chief, with the assistance of Di Long, Associate Editor

Keywords:
Seepage meters
Differential streamflow gauging
Hydrograph separation
Measurement uncertainty
Groundwater discharge

ABSTRACT

The groundwater contribution to streamflow along a lowland alluvial stream in Denmark was estimated using a variety of methods and at different spatial scales. At the point-scale (less than a few metres), groundwater discharge to the stream was measured using seepage meters. At the reach-scale (0.5–1.5 km), groundwater discharge to the stream was estimated using differential streamflow gauging. And at the catchment-scale (> 1.5 km), groundwater discharge to the stream was estimated using hydrograph separation. The estimates of groundwater discharge obtained using point-scale measurements range from 12 to 41 cm/d which is lower than fluxes estimated at the reach-scale which range from 18 to 333 cm/d. This discrepancy was attributed to the partitioning of groundwater discharge into streambed seepage and bank seepage. On the other hand, the groundwater discharge estimates obtained using hydrograph separation were generally the highest and ranged from 194 to 289 cm/d. For this study, this discrepancy from the reach-scale estimates was attributed to the assumption that baseflow obtained using hydrograph separation represents groundwater discharge to the stream when part of the baseflow actually comes from artificial drainage systems. Anyhow, seepage meter measurements, differential streamflow gauging, and hydrograph separation showed similar trends. The increase in streamflow is mainly due to either groundwater discharge through the streambed and the banks in the lower part, or tile drainage discharge in the upper part of the catchment. Furthermore, estimation of uncertainty for the various groundwater discharge estimates showed that some of the flux estimates were insignificant compared with their propagated uncertainties. To this end, a novel method was developed to estimate the uncertainty of groundwater discharge estimates obtained by hydrograph separation. Overall, this paper shows that more than one method should be used to obtain a reliable estimate of groundwater discharge to a lowland alluvial stream from other discharge contributions such as tile drainage.

1. Introduction

Most streams in Denmark flow year-round and are located in humid lowland alluvial areas with a thin unsaturated zone. Thus, the groundwater and surface water systems are strongly interconnected, and groundwater is an important component of total streamflow in many of these streams (e.g. van Roosmalen et al., 2007). In such interconnected systems, groundwater withdrawals can deplete streamflow (e.g. Nyholm et al., 2002) with detrimental consequences for stream ecosystems (e.g. Johansen et al., 2011). In addition to water-budget concerns, it is also of importance to assess the water fluxes between groundwater and surface water because of the risk of excess nutrients leaching to aquifers and streams, especially in agricultural catchments (Kronvang et al., 2005), which constitute approximately two thirds of all land in Denmark. It is well known that the potential for reducing nitrate via denitrification and thus improvement of water quality depends on where and how groundwater discharges to alluvial streams. Therefore, reliable methods for estimating groundwater discharge to streams are needed for successful water-resource management.

Common methods used to estimate groundwater discharge are reviewed by for example Kalbus et al. (2006) and include seepage meter measurements (e.g. Lee, 1977; Rosenberry, 2008), natural tracer methods (e.g. Xie et al., 2016), heat tracer methods (e.g. Anderson, 2005; Constantz, 2008; Hatch et al., 2006; Lowry et al., 2007), mass balance approaches including differential streamflow gauging (e.g. Cey et al., 1998; Harte and Kiah, 2009; Langhoff et al., 2006; Schmadel et al., 2010) and hydrograph separation (e.g. Gonzales et al., 2009; Hannula et al., 2003). Generally, these methods may be divided into three groups: those that estimate the groundwater flux directly through

* Corresponding author.
E-mail address: rasmus.rumph@geo.au.dk (R.R. Frederiksen).

https://doi.org/10.1016/j.jhydrol.2018.07.036
Received 22 December 2017; Received in revised form 15 May 2018; Accepted 14 July 2018
Available online 17 July 2018

the sediment-water interface at point-scale (less than a few metres); those that estimate the volumetric change in flow along the stream at reach-scale (100 m to several kilometres); and those that estimate the integrated response of the surface-groundwater interaction at catchment-scale (greater than a few kilometres). Although, it is well known that the processes governing the groundwater discharge estimate are different depending on the method (Cranswick and Cook, 2015; Kalbus et al., 2006), it is relevant and important to compare these results because the interpretation of the importance of groundwater discharge to the stream-water budget would be greatly dependent on the method used for quantifying the input (e.g. Becker et al., 2004).

At the point-scale, direct measurements of water flux across the sediment-water interface by seepage meters are widely applied in streams. The seepage meter relies on a simple concept and is inexpensive to construct. However, since the meter covers a relatively small bed area, its application can be influenced by streambed heterogeneity and measurements at many locations are therefore required with large associated labour costs. Numerous studies have addressed this by combining seepage meters with fibre optic distributed temperature sensing (e.g. Rosenberry et al., 2016). Furthermore, seepage meters measure the water exchange across the streambed, while other components of the total groundwater discharge are neglected, including seepage through the banks. This component, however, can be measured with alternative seepage meters (Langhoff et al., 2006). On the other hand, water flux across the sediment-water interface measured with seepage meters may include a contribution from hyperheic flow in addition to the groundwater contribution (e.g. Rosenberry and Pitlick, 2009).

At the reach-scale, closely spaced measurements of streamflow referred to as differential streamflow gauging can estimate the net groundwater flux to streams through the bed and the banks if all other fluxes in and out of the reach are accounted for (Cey et al., 1998; Harte and Kiah, 2009; Langhoff et al., 2006; Opsahl et al., 2007; Schmadel et al., 2010). Results of for example Cey et al. (1998) suggest that differential streamflow gauging gives more reasonable estimates of the groundwater discharge contribution to streamflow than point-scale estimates.

At the catchment-scale, the quintessential method to estimate the groundwater contribution to streams is hydrograph separation which has a long history in hydrology (Gonzales et al., 2009; Hall, 1968; Tallaksen, 1995). Basically, a stream hydrograph is separated into a short-term fluctuating component (typically named "direct runoff") and a long-term fluctuating component (typically named "baseflow"). It is then assumed that baseflow represents groundwater discharge to the stream.

Hydrograph separation methods can be divided into tracer-based and non-tracer based. Results of Gonzales et al. (2009) suggest that tracer-based hydrograph separation methods provide the hydrological most reasonable estimates of the groundwater contribution to streamflow in a lowland catchment. However, tracer-based hydrograph separation methods are more costly and labour-intensive than non-tracer based methods, and long-term tracer data are not available from most gauging stations. Therefore, it is important to evaluate the ability of non-tracer based hydrograph separation methods to give reasonable estimates of groundwater discharge despite the limitations of such techniques. Gonzales et al. (2009) suggest that the rating curve/envelope method (Kliner and Knezek, 1974; Sellinger, 1996) and the recursive filter methods (Eckhardt, 2005) are the best to estimate the groundwater contribution to streamflow. However, these methods require groundwater level measurements and calibration to tracer-based results, respectively.

A limitation of non-tracer based hydrograph separation methods is that the identification of the groundwater component of continuous discharge data is uncertain because other inputs such as tributaries, overland flow and tile drainage systems may exceed the groundwater discharge and cause a similar recession (e.g. Halford and Mayer, 2000). Therefore the groundwater discharge is easily overestimated by hydrograph separation methods. One may overcome this by estimating the water balance between two gauging stations on the same stream system taking into account major inputs and losses (McCallum et al., 2014; Opsahl et al., 2007; Sutton et al., 2014).

The first objective of this study is to characterise the groundwater discharge to a 4.8 km long lowland alluvial stream in the western part of Denmark based on an application of methods at point-, reach-, and catchment-scale. The methods of groundwater discharge estimation are: (1) seepage meter measurements at the point-scale, (2) differential streamflow gauging at the reach-scale, and (3) hydrograph separation at the catchment-scale. The second objective is to compare and discuss the groundwater discharge estimates obtained by these various methods working on different spatial scales. To support this comparison and discussion, we estimate the standard deviations and confidence intervals associated with the various flux estimates. To this end, we develop a novel method to estimate the uncertainty of groundwater discharge estimates obtained by hydrograph separation.

For clarity, in hydrological systems such as the one studied here water can flow to a stream (1) directly through the streambed and the banks (referred to as groundwater discharge), (2) diffusively to the riparian zone from where it discharges to the stream at locations where ponded water spills over the bank into the stream channel (overland flow), and (3) through drain pipes or ditches bypassing the riparian area aquifer and discharging to the stream (tile drainage discharge) (Dahl et al., 2007; Langhoff et al., 2006). The various methods used in this paper measure or estimate one or more of these streamflow components.

2. Site description

The Knivsbaek catchment is located in the western part of Denmark (Fig. 1) inside the Hydrological Observatory – Skjern Catchment (HOBE) (Jensen and Illangasekare, 2011). To the west, Knivsbaek catchment is bounded by an ice-pushed moraine called Fjaldene (topographic divide). To the south it is bounded by valley terraces separating the stream from the town Videbaek. To the north and east, it is bounded by Abildaa stream. The area of the topographical catchment is 12.4 km^2.

The groundwater divide in Fig. 1 was based on hydraulic head data from 48 wells in the area. In most of the wells, hydraulic head was measured once, shortly after the well construction, or twice – at the year of the well construction, as well as during a field campaign on 6–10 April 2015 (only 17 boreholes available for measurement). The groundwater catchment is smaller than the topographical catchment toward the west and northwest. On the other hand, it coincides with the topographical divide in the lower parts of the study area to the east, while in some places to the south it is beyond the topographical divide.

The highest part of the catchment at the Fjaldene moraine reaches near 85 masl. It is characterized by sandy permeable soils on top of tills. At the bottom of the moraine to the east, the catchment becomes flat, with altitudes between 30 and 35 m above sea level. Here, the lithology consists of either glacial outwash sand and gravel of Quaternary age on top of alternating layers of Miocene mica clay (referred to as cover layer in Fig. 1), or Miocene sand (Rasmussen et al., 2010) overlain by peat in the lowest areas to the east (Frederiksen et al., 2017). The thickness of the Quaternary deposits varies from 1 m to up to approximately 10 m (Frederiksen et al., 2017). The reader is referred to Frederiksen et al. (2017) for a detailed description of the shallow geology.

The drainage system is dense in parts of the study area as is typical for Danish lowland alluvial areas (Fig. 1). It consists of open ditches and tile drain pipes that were implemented to maximize crop growth by lowering the shallow groundwater table. The drainage system has been made where either low permeable deposits are shallow, or the groundwater table is shallow because of the topography being both flat and low. Confluence points between drainage tile outlets and Knivsbaek

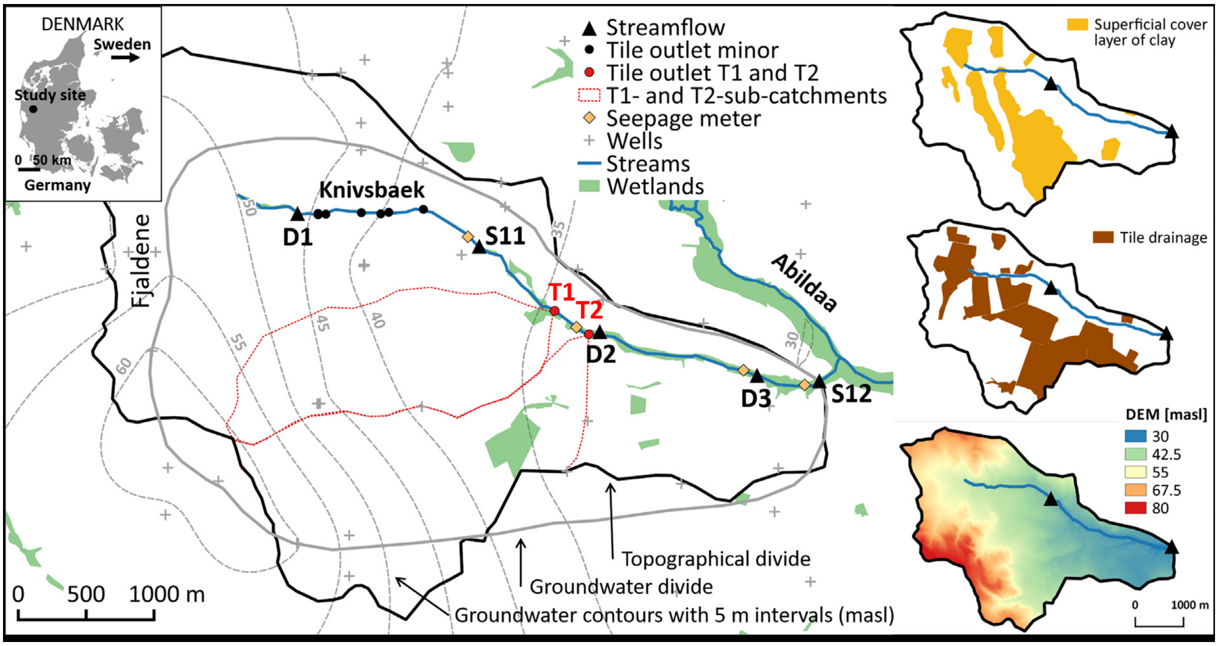

Fig. 1. The study site Knivsbaek in western Denmark. S11 and S12 are stream gauging stations. Streamflow measurements were taken at D1, S11, D2, D3 and S12. T1 and T2 are the two largest tile drainage outlets. Reach 1 is from D1 to S11, reach 2 is from S11 to D2, reach 3 is from D2 to D3, and reach 4 is from D3 to S12.

stream are indicated in Fig. 1.

Knivsbaek stream, which flows year-round, originates in a wetland in the west of the catchment and flows 4800 m to the east with a mean gradient of approximately 0.004 through agricultural fields before reaching the outlet station at S12. Approximately 2500 m downstream from the source of Knivsbaek, the wetland and riparian meadows around the stream widens from a few meters to 50–100 m. Along the stream, drainage water enters the stream at eight locations: six tile drain outlets from the fields in the upper part of the catchment; and two tile drain outlets between 2500 m and 2300 m downstream from the fields in the southern part of the catchment (T1 and T2 in Fig. 1). During baseflow conditions the width of Knivsbaek stream ranges from 0.5 to 3 m and the depth from 10 to 50 cm, but during high-flow events depths up to 1.5 m occur. The streambed consists of coarse sand and gravel, but thin silt deposits and organic material are present where water moves slowly.

The Knivsbaek catchment is divided into two sub-catchments by the two automated gauging stations, S11 and S12, and the stream is further sub-divided into four reaches as follows: reach 1 from D1 to S11, reach 2 from S11 to D2, reach 3 from D2 to D3, and reach 4 from D3 to S12 (Fig. 1).

3. Material and methods

3.1. Continuous stream discharge data

Stream stage was recorded every 15 min from 1 November 2014 to 31 October 2016 at upstream (S11 in Fig. 1) and downstream (S12 in Fig. 1) locations using pressure transducers (Type: Schlumberger Mini-Diver Water Level and Temperature Sensor) installed in stilling wells. Furthermore, at each gauging location, stream discharge was measured sub-monthly during both high and low flows following the recommendations of Herschy et al. (1999) and using hydrometric propellers (Type: OTT, C31 Universal Current Meter). Discharge was calculated using the velocity-area technique. The standard deviation for such a discharge estimate in this type of stream is approximately 5% (Ovesen, 2011).

The stage discharge data were used to develop rating curves for both stations (Herschy et al., 1999). The rating curves were generated using HYMER (www.orbicon.com). HYMER is a hydrometric software package that manages hydrometric, hydrological and climate data and allows continuous correction of variations in channel roughness due to weed growth during spring and summer. The rating curves provided a theoretical baseline for estimating 15-minute incremented time series of stream discharge as well as a series of daily average discharge values. The standard deviation for such data in this type of environment is assumed to be 20%, which is similar to the standard deviation for stage-based stream discharge data in two other HOBE sub-catchments (Holtum and Ahlergaarde) based on expert elicitation (Sebok et al., 2016). The daily discharge data were used for differential streamflow gauging over time and hydrograph separation, respectively, as described below. The specific stream discharge ($ls^{-1} km^{-2}$) was calculated by dividing discharge with the topographic area of the catchment.

3.2. Groundwater discharge estimates

3.2.1. Seepage meter measurements

Groundwater discharge through the streambed was measured using 660 cm^2 circular seepage meters (Lee, 1977) at four locations along the stream on 15 April and 6 August 2015. The seepage cylinder was connected via a 1 m flexible plastic tube to a partly pre-filled 4 l plastic collection bag sheltered to minimize the effect of velocity-head effects associated with moving water (Rosenberry, 2008). After a pre-set time interval, the bag was removed and the volume of water collected was measured in order to calculate a seepage rate. Two separate measurements were made at each seepage meter installation with a temporal gap of eight hours to ensure that plenty of time was given for the system to return to normal before the second measurement. Three seepage meters were installed and measured simultaneously at each location to minimize concerns about local-scale heterogeneity, and the local groundwater flux was estimated as the average of the six seepage meter measurements.

Water flux measured using a seepage meter is commonly multiplied by a correction factor to account for the total flow-resistance in the meter including barrel, outlet, tube, valves and collection bag (Rosenberry, 2005). The correction factor may vary from 1.05 (Rosenberry, 2005) to 1.74 (Erickson, 1981). In the present study precautions were taken in applying the meter, and a factor of 1.10 was used.

3.2.2. Detailed differential streamflow gauging

Detailed differential streamflow gauging was taken on 15 April and 6 August 2015. Here streamflow was measured using an Ott-C31 propeller at five locations (D1, S11, D2, D3 and S12 in Fig. 1). At the same time, discharge from all tile drain outlets and all overland flows were measured between D1 and S12 (Fig. 1); they were measured using an Ott-C2 mini-propeller where possible, otherwise by a plastic bag and a stopwatch. Using a water balance and accounting for all fluxes in and out of the reach, the groundwater discharge for each of the four reaches was estimated as

$$Q_{gw} = Q_{down} - Q_{up} - Q_{in} \quad (1)$$

where Q_{down} and Q_{up} are streamflow at the downstream and upstream end of the reach, respectively, and Q_{in} is the sum of flow into the reach from tile drain outlets and overland flow. Using (1) it is implicitly assumed that change in channel storage and losses due to for example evapotranspiration are negligible.

Streamflow gain, tile drainage discharge and overland flow are measured values, while groundwater discharge is a residual value estimated as streamflow gain subtracted tile drainage discharge and overland flow. That is, groundwater discharge is defined here as flow from the groundwater system to the stream directly through the streambed or through the banks. Groundwater discharge was divided by the streambed area to give estimates of groundwater discharge flux (cm/d).

3.2.3. Differential streamflow gauging over time

Significant tile drainage discharge and overland flow contributions to stream flow between gauging station S11 and S12 can be limited to the two largest tile drain outlets, T1 and T2 (Fig. 1). Again neglecting change in channel storage and loss from evapotranspiration, the mean daily groundwater discharge between S11 and S12 was estimated as

$$Q_{diff}(t) = Q_{12}(t) - Q_{11}(t) - Q_T(t) \quad (2)$$

where $Q_{12}(t)$ and $Q_{11}(t)$ are mean daily streamflow at S12 and S11, respectively, and $Q_T(t)$ is the sum of inflow from T1 and T2 (Fig. 1).

Unfortunately, we were unable to continuously monitor inflows from T1 and T2. Instead, we established a correlation between streamflow at S11 and the sum of inflow from T1 and T2 by conducting a number of flow measurements at these locations between August 2015 and February 2016. The measurements are shown in Fig. 2. The correlation between streamflow at S11 and the sum of inflow from T1 and T2 is 1:1 or 1:1.8 when streamflow at S11 is below or above, respectively, 80 l/s.

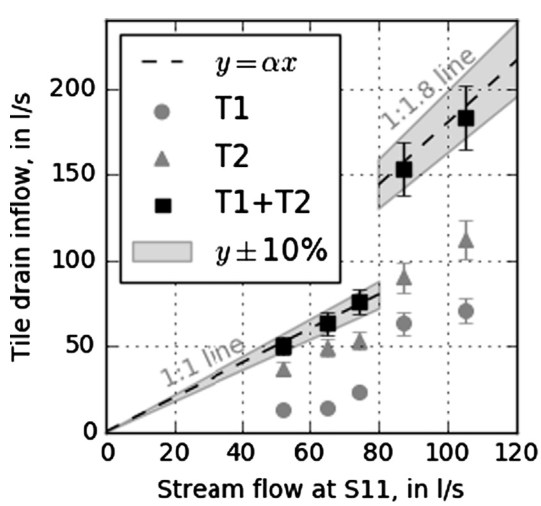

Fig. 2. A comparison of streamflow at S11 (l/s) and tile drain inflow from T1 and T2 (l/s) (see Fig. 1).

Using these correlations, $Q_{diff}(t)$ can be estimated from mean daily streamflow at S12 and S11, respectively, as

$$Q_{diff}(t) = Q_{12}(t) - \alpha \times Q_{11}(t) \quad (3)$$

where the constant α is

$$\alpha = \begin{cases} 2 & \text{for } Q_{11}(t) \le 80 \text{ l/s} \\ 2.8 & \text{for } Q_{11}(t) > 80 \text{ l/s} \end{cases} \quad (4)$$

3.2.4. Hydrograph separation

The continuous discharge data for gauging stations S11 and S12 were separated into baseflow and direct runoff using the United Kingdom Institute of Hydrology method (UKIH method) which is widely used since it is easy to apply and it is a standardized and systematic filtering method (Gustard et al., 1992). A Python script was used to carry out the procedure. The script divides the daily stream discharge data into 5-day non-overlapping blocks of data. For each block of data, the script calculates the discharge minima of five-day non-overlapping consecutive periods, and subsequently searches for turning points in this sequence of minima. Turning points are defined as minima that are smaller than their neighbouring minima when multiplied by 0.9. The turning points are then connected to obtain the baseflow hydrograph which is constrained to equal the observed hydrograph ordinate on any day when the separated hydrograph exceeds the observed. The direct runoff ratio was calculated as direct runoff divided by total discharge.

Assuming that baseflow represents groundwater discharge to the stream, the mean daily groundwater discharge between S11 and S12 was estimated as

$$QB_{diff}(t) = QB_{12}(t) - QB_{11}(t) \quad (5)$$

where $QB_{12}(t)$ and $QB_{11}(t)$ are mean daily baseflow at S12 and S11, respectively, calculated using the UKIH method.

3.3. Uncertainty estimation

The following subsections explain how the standard deviation, SD, was determined for various flow estimates, Q. In the results section and discussion section each Q is presented with its 95% confidence interval. The confidence interval was calculated simply as$Q \pm 2 \times SD$.

3.3.1. Seepage meter measurements

Simple statistics (mean and standard deviation) were calculated for groundwater discharge estimates obtained using seepage meters. The values were based on data from six seepage measurements at each location (orange dots in Fig. 1).

3.3.2. Detailed differential streamflow gauging

Assuming that measurement uncertainties of Q_{down}, Q_{up}, and Q_{in} in (1) are independent, the standard deviation for groundwater discharge estimates obtained using detailed differential streamflow gauging was calculated using uncertainty propagation as

$$SD_{Qgw} = \sqrt{SD_{Qdown}^2 + SD_{Qup}^2 + SD_{in}^2} \quad (6)$$

where SD_{Qdown} and SD_{Qup} are standard deviations for streamflow at the downstream and upstream end of the reach, respectively, while SD_{Qin} is the standard deviation for the sum of flow into the reach from tile drain outlets and overland flow. In the present case, using (6) it is assumed that the standard deviation for the sum of flows into the reach from tile drain outlets and overland flow is 10% of their total flow rate; for each of the stream flows the standard deviation is 5% of the flow rate (Ovesen, 2011).

3.3.3. Differential streamflow gauging over time

Assuming that measurement uncertainties of Q_{12} and Q_{11} in (3) are independent, the standard deviation for $Q_{diff}(t)$ was calculated using uncertainty propagation as (Goodman, 1960)

$$\boldsymbol{SD_{Qdiff}} = \sqrt{\boldsymbol{SD}_{Q12}^2 + \boldsymbol{Q}_{Q11}^2\boldsymbol{SD}_{\alpha}^2 + \alpha^2\boldsymbol{SD}_{Q11}^2} \tag{7}$$

where SD_{Q12} and SD_{Q11} are standard deviations for daily stream discharge at S12 and S11, respectively, and SD_α is standard deviation of the constant α.

Calculating SD_α as the standard deviation of the estimated slope of the two regression lines with known intercept in Fig. 2 is problematic because of the low number of measurements. Estimating SD_α this way gave an unreasonable low deviation (2% and 0.6% for $\alpha = 2$ and $\alpha = 2.8$, respectively). However, a somewhat higher value for SD_α is expected if more measurements had been available. Therefore, using (7) it is instead assumed that SD_α amounts to 10% (grey shaded area in Fig. 2).

3.3.4. Hydrograph separation

Assuming that measurement uncertainties of QB_{12} and QB_{11} in (5) are independent, the standard deviation for $QB_{diff}(t)$ was calculated using uncertainty propagation as

$$\boldsymbol{SD_{QBdiff}} = \sqrt{\boldsymbol{SD}_{QB12}^2 + \boldsymbol{SD}_{QB11}^2} \tag{8}$$

where SD_{QB12} and SD_{QB11} are standard deviation for baseflow at S12 and S11, respectively.

Each of SD_{QB12} and SD_{QB11} were calculated for 5-day non-overlapping blocks of data containing 15 April 2015 and 6 August 2015, respectively. To this end, a novel method was developed. For example, to calculate SD_{QB11} for the 5-day non-overlapping block containing 6 August 2015 (referred to as SD_{QB11_AUG}) the following procedure was used:

1. Divide the daily stream discharge data for gauging station S11 into 5-day non-overlapping blocks of data. For each block, compute the mean and standard deviation of the corresponding set of data; let the mean and standard deviation for block i be called x_i and s_i, respectively. (A scatter point in Fig. 3 represents the mean and standard deviation for a specific block of data.)
2. Let the mean for the 5-day block containing the data for 6 August 2015 be called x_0 (indicated by dotted line in Fig. 3).
3. Calculate the mean of s_i for all the blocks of data (all the points in Fig. 3) which satisfy that $|x_i - x_0| < 0.1x_0$ (grey shaded area in Fig. 3), and let this mean value be called s_0. This measures the typical scatter of data having a block mean value of x_0, which is the average stream discharge in the five day period of 6 August 2015.
4. Set SD_{QB11_AUG} equal to s_0.

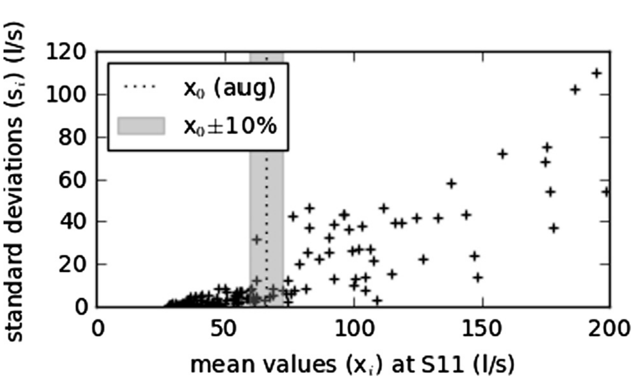

Fig. 3. Mean values and standard deviations for the continuous discharge at gauging station S11 (l/s) for each 5-day non-overlapping block used in the UKIH-procedure (scatter points), as well as the mean for the 5-day block containing 6 August 2015 (dotted line).

Table 1
Groundwater discharge estimates obtained using seepage meter measurements at four locations (25 m upstream S11, D2, D3, and S12). Values are based on data from six seepage meter measurements at each location.

Location	Mean flux, cm/d	Estimated 95% confidence interval, cm/d
Seepage meter measurements 15 April 2015		
S11	15	± 6
D2	12	± 15
D3	32	± 22
S12	41	± 16
Seepage meter measurements 6 August 2015		
D2	17	± 7
D3	40	± 38

4. Results

4.1. Seepage meters

Seepage meter measurements of groundwater discharge were taken at four locations (25 m upstream S11, D2, D3 and S12, respectively; see Fig. 1) along the stream on 15 April 2015 and at two locations (D2 and D3) on 6 August 2015. The results are presented in Table 1. The measured groundwater fluxes were upwards at all locations and tend to increase from upstream to downstream. The values range from 12 ± 15 to 41 ± 16 cm/d with an insignificant difference between 15 April and 6 August.

It was observed that the six seepage measurements taken at each location resulted in large 95% confidence intervals (Table 1), even though the streambed sediments at all four locations appear to consist of homogeneous coarse sand and gravel.

4.2. Detailed differential streamflow gauging

On 15 April and 6 August 2015, streamflow was measured at five locations (D1, S11, D2, D3 and S12 in Fig. 1) along the stream, together with discharge from tile drainage outlets and overland flow (tile drainage outlets are shown on Fig. 1). No precipitation occurred for 4 days prior to the August measurements and the streamflow hydrograph indicates low and constant stream discharge (Fig. 5). On the other hand, the April measurements were taken after a wet period. On this basis, it is assumed that the August measurements represent a "dry" groundwater system with relatively low groundwater levels, low soil water content and empty shallow runoff reservoirs, while the April measurements represent a "wet" system. The results are presented in Table 2.

On 15 April and 6 August, the groundwater discharge along the entire stream length, is estimated to be 77 l/s (52% of the streamflow gain) and 44 l/s (50%), respectively. However, the relative importance of tile drainage discharge, overland flow and groundwater discharge varies along the stream. On 15 April, tile drainage discharge accounted for 79% of the increase in streamflow along reach 1, 94% along reach 2, 9% along reach 3 and 0% along reach 4, while overland flow accounted for 0%, 0%, 3% and 42%, respectively. Hence, groundwater discharge along each of the reaches accounted for 21%, 6%, 88% and 58%, respectively. This pattern was evident on 6 August as well. On this basis, reaches 1–2 can be classified as tile drainage dominated, while reaches 3–4 are groundwater dominated.

It is noticed that the confidence interval is very wide for the estimates of groundwater discharge, and especially for reaches 1, 2, and 4 (Table 2). The wide intervals are mainly caused by uncertainty of the streamflow gain from which the groundwater discharge is estimated (can be deducted from the numbers given in Table 2).

Moreover, an inspection of stream physical characteristics for reach 1 through 4 reveals that the average stream width increases from 0.65 m to 0.93 m, 1.20 m and 1.45 m, respectively, while the average

Table 2
Differential streamflow gauging on 15 April and 6 August 2015, and reach characteristics.

	Reach 1	Reach 2	Reach 3	Reach 4
Differential streamflow gauging 15 April 2015				
†Streamflow gain (l/s)	14 ± 7	48 ± 12	68 ± 20	19 ± 26
†Tile drainage discharge, in l/s (%)	11 ± 2 (79)	45 ± 9 (94)	6 ± 2 (9)	0
†Overland flow, in l/s (%)	0	0	2 ± 0 (3)	8 ± 2 (42)
*Groundwater discharge, in l/s (%)	3 ± 7 (21)	3 ± 15 (6)	60 ± 20 (88)	11 ± 26 (58)
**Groundwater discharge, in cm/d	28 ± 67	27 ± 132	333 ± 110	135 ± 315
Differential streamflow gauging 6 August 2015				
†Streamflow gain (l/s)	14 ± 4	34 ± 8	33 ± 13	7 ± 15
†Tile drainage discharge, in l/s (%)	12 ± 2 (86)	32 ± 6 (94)	0	0
†Overland flow, in l/s (%)	0	0	0	0
*Groundwater discharge, in l/s (%)	2 ± 5 (14)	2 ± 10 (6)	33 ± 13 (100)	7 ± 15 (100)
**Groundwater discharge, in cm/d	18 ± 46	18 ± 94	183 ± 73	83 ± 183
Reach characteristics				
Stream length, in m	1450	1050	1300	500
Stream width avg, in m	0.65	0.93	1.20	1.45
Wet riparian area, in m^2	0	50,370	67,040	41,520
Wet riparian width avg, in m^2	0	48	52	83
Wet riparian area (% of sub-catchment area)	0.0	1.0	4.7	8.3
Reach classification	Tile drainage dominated	Tile drainage dominated	Ground-water dominated	Ground-water dominated

For tile drainage discharge, overland flow, and groundwater discharge, the percentage of total streamflow gain is given in parenthesis.
† Streamflow gain, tile drainage discharge and overland flow are measured values.
* Groundwater discharge is a residual value estimated as streamflow gain subtracted tile drainage discharge and overland flow. Thus, groundwater discharge is defined here as flow from the groundwater system to the stream directly through the streambed or the banks.
** Groundwater discharge was divided by the streambed area to give estimates of groundwater discharge in cm/d.

wet riparian width increases from 0 m to 48 m, 52 m and 83 m, respectively. Furthermore, the wet riparian area constitutes 0%, 1.0%, 4.7% and 8.3% of the four sub-catchments. That is, the two groundwater dominated reaches have wider stream channels and wider wet riparian areas than the two tile drainage discharge dominated reaches. These characteristics are therefore consistent with the results of the detailed differential streamflow gauging.

4.3. Differential streamflow gauging over time

Between gauging stations S11 and S12, mean daily groundwater discharge was estimated using continuous discharge data for S11 and S12 (black line in Fig. 4). For April through September, mean monthly groundwater discharge varied from 100 ± 60 cm/d to 160 ± 120 cm/d with June and July having the lowest values. On 15 April and 6 August 2015, the fluxes were estimated to be 161 ± 96 and 108 ± 54 cm/d, respectively (red vertical lines in Fig. 4).

Overall, the groundwater discharge is relatively constant during the period shown in Fig. 4. However, the stream reach between S11 and S12 is located in a low lying area where high stream stage at high stream discharge potentially may reverse the hydraulic gradient over the sediment-water interface for shorter periods. For example, the two large negative peaks that occurred start June and end July are likely examples of flux reversals. Pressure transducers or temperature loggers placed in the water column and streambed in different depths could test this hypothesis.

4.4. Hydrograph separation

For gauging stations S11 and S12, the daily precipitation and stream discharge data show an immediate response of runoff to precipitation events, and short recession curves indicate that fast runoff reservoirs are present (Fig. 5A). For S11 and S12, the annual mean specific stream discharge is approximately 13 $l s^{-1} km^{-2}$ and 17 $l s^{-1} km^{-2}$, respectively (Fig. 5B). Typical values for streams in western Denmark are 13 $l s^{-1} km^{-2}$ (Ovesen et al., 2000). For S11 and S12, the annual variation of monthly mean specific stream discharge ranges from 7 to 26 $l s^{-1} km^{-2}$ and 10 to 30 $l s^{-1} km^{-2}$, respectively, with values above the annual mean from November to March and below from April to October. For both S11 and S12, the flow duration curves show a portion of small daily discharges (dry summer days) and a portion of large daily discharges (wet winter days and large summer precipitation events) (Fig. 5C). S11 has a higher portion of small values than S12 and some very large values ($> 60\ l s^{-1} km^{-2}$) not observed at S12.

For gauging stations S11 and S12, the continuous discharge data were separated into baseflow and direct runoff using the UKIH method (Fig. 6A and B, respectively). For S11 and S12, the annual mean direct runoff ratio is 0.26 and 0.21, respectively (Fig. 6C). For both stations, the monthly mean direct runoff ratio varies over the year having values above annual mean in September and from November through January, while having values less than 0.10 in May, August and October. For S11 and S12, values during the year range from 0.05 to 0.43 and 0.04 to 0.34, respectively. S11 has higher monthly mean direct runoff ratios

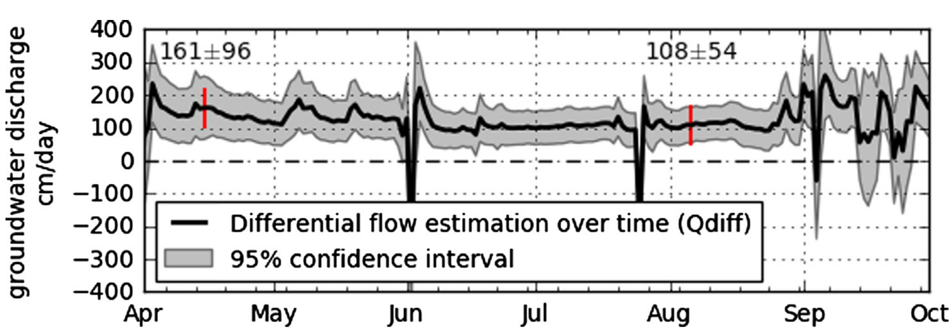

Fig. 4. Mean daily groundwater discharge (cm/d) estimated from measured continuous discharge data for April 2015 through September 2015. The associated 95% confidence interval is shown as the grey band. Red vertical lines show location of 15 April and 6 August 2015. (For interpretation of the references to colour in this figure legend, the reader is referred to the web version of this article.)

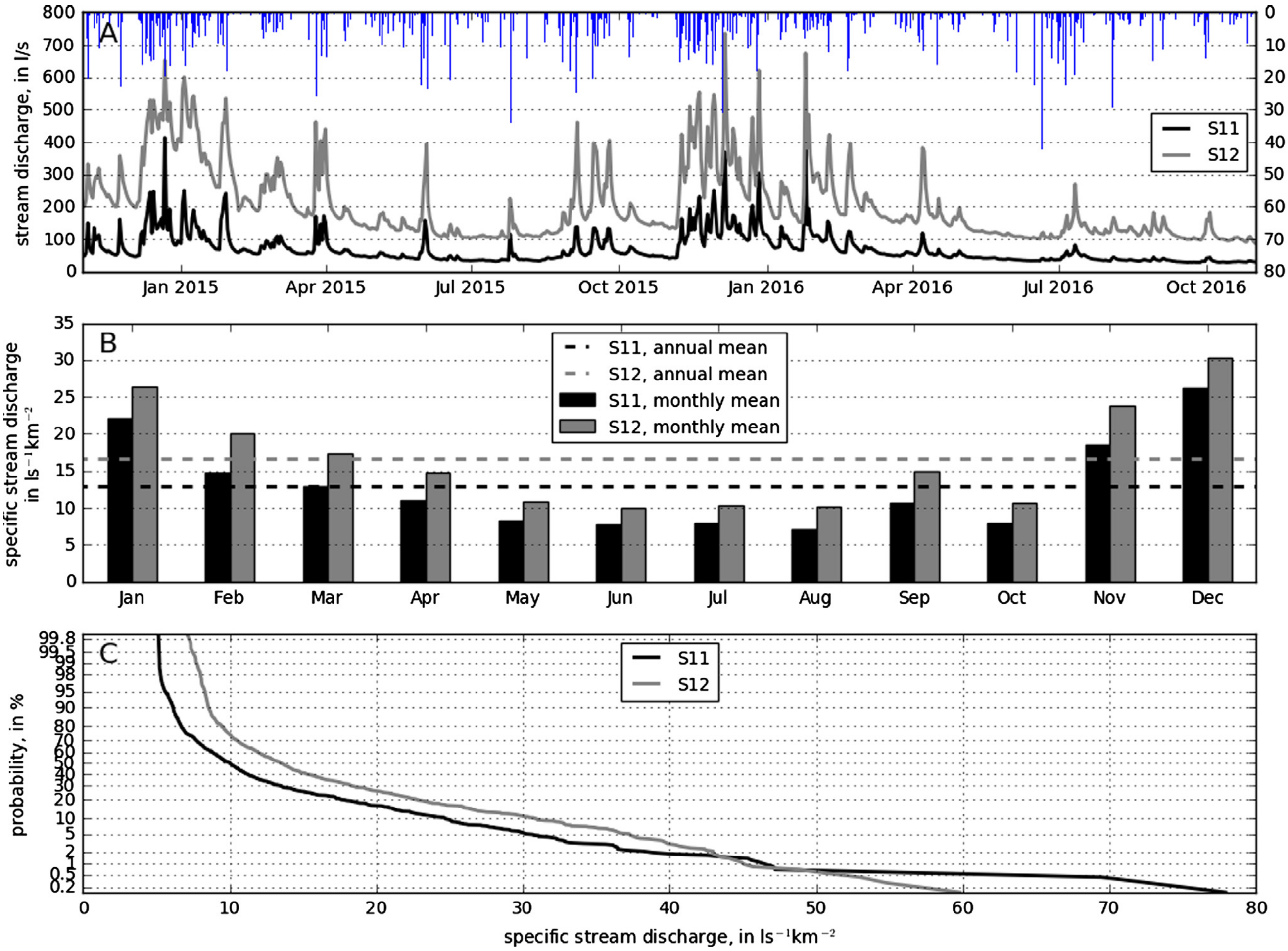

Fig. 5. For gauging stations S11 and S12 for the period from 01-Nov-2014 to 31-Oct-2016: (A) daily precipitation (mm/d) and daily mean discharge (ls^{-1}), (B) annual and monthly mean specific stream discharge ($ls^{-1}km^{-2}$), and (C) flow duration curve (%) for specific stream discharge ($ls^{-1}km^{-2}$).

than S12 for months with above-annual-mean ratio, while the ratio for the two stations is more similar for all other months.

Furthermore, between gauging stations S11 and S12 mean daily groundwater discharge was estimated using daily baseflow values for S11 and S12. On 15 April and 6 August 2015, the groundwater discharge fluxes over this stream reach were 289 ± 102 and 194 ± 31 cm/d, respectively.

5. Discussion

5.1. Groundwater discharge along Knivsbaek stream

Streamflow observations at two gauging stations within the Knivsbaek catchment revealed a fast response to precipitation events in the studied lowland alluvial area. The corresponding flow duration curves (Fig. 5C) show that the upstream gauging station (S11 in Fig. 1) has a larger portion of small specific stream discharge values and more very large values than the outlet gauging station (S12 in Fig. 1). Furthermore, the relative contribution of the mean annual direct runoff component to the streamflow hydrograph is approximately 25% larger for S11 than for S12. These findings indicate that groundwater discharge is less important for streamflow at S11 than for streamflow at S12.

The specific stream discharge is approximately 30% larger for S12 than for S11 throughout the observation period (Fig. 5B). This indicates that groundwater may be recharged in the upland parts of Knivsbaek catchment, flow to lower lying areas to the east, and discharge directly to Knivsbaek stream or its surrounding riparian areas. As explained in the site description, the groundwater catchment is likely to be smaller than the topographical catchment toward the west and northwest and therefore Knivsbaek catchment may be losing a likely small amount of groundwater to neighbouring catchments to the west of the topographical highs of Fjaldene. This is confirmed by the groundwater level contours in Fig. 1. The general groundwater flow pattern combined with the spatial differences between groundwater divide and topographical divide is likely to explain why specific stream discharge values for S12 are larger than those for S11, even though the S11-subcatchment is part of the catchment to S12.

Groundwater discharge measured using seepage meters showed that flux through the streambed to the upper reaches (reaches 1–2) is 50% of the flux to the lower reaches (reaches 3–4). Groundwater discharge estimated using detailed differential streamflow gauging showed that flux through the streambed and the banks to the lower reaches is 4 to 10 times larger than the flux to the upper reaches. The general groundwater flow pattern is likely to explain this spatial difference in groundwater discharge.

The hydrogeological controls on increase in streamflow vary along the stream. The increase in streamflow along reaches 1–2 (D1 to S11 and S11 to D2, respectively, in Fig. 1) is mainly due to tile drainage discharge (79–94%, in Table 2). The agricultural fields around reach 1 are artificially drained because the groundwater table is shallow where the topography transitions from high hills to a flat stream valley (Fig. 1). Tile drainage discharge via T1 and T2 (Fig. 1) accounts for approximately 94% of the increase in streamflow along reach 2 (Table 2). T1 and T2 drain the low lying areas to the south where superficial low permeable deposits are present. On the other hand, the

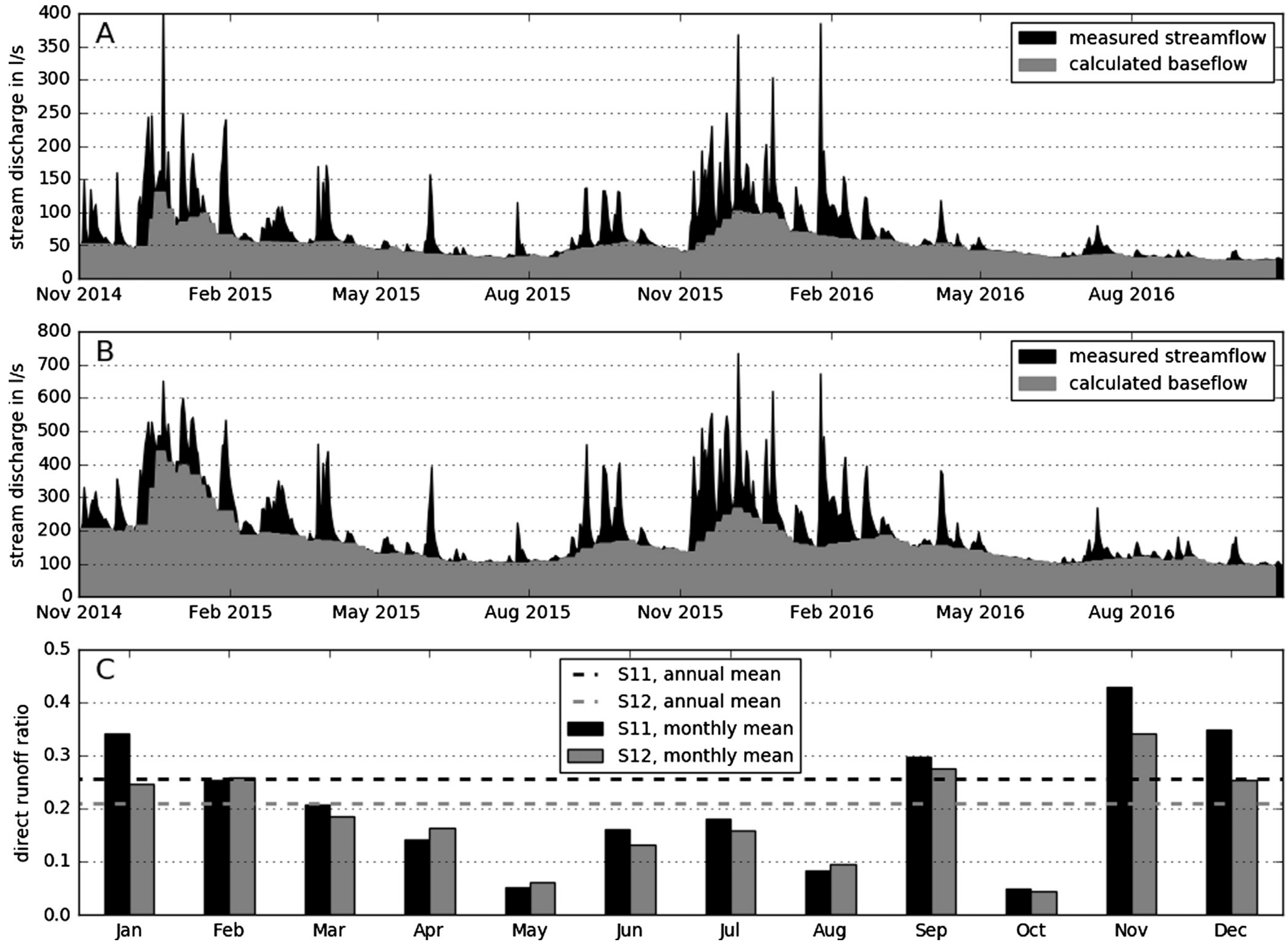

Fig. 6. Results from hydrograph separation: total stream discharge (l/s) and baseflow (l/s) for gauging stations S11 (A) and S12 (B), and annual and monthly mean direct runoff ratio for gauging stations S11 and S12 (C).

increase in streamflow along reaches 3–4 (D2 to D3 and D3 to S12, respectively, in Fig. 1) is mainly due to groundwater discharge (58–100%, in Table 2) which may be controlled by the catchment-scale groundwater flow direction combined with flat low-lying areas and high permeable sediments in this part of Knivsbaek catchment (Fig. 1). In order to facilitate the larger groundwater discharge in the lower part of the catchment, the riparian areas next to the stream are wider and the stream channel is wider. The wide riparian area also makes some groundwater discharge to the most downstream reaches as overland flow (Table 2).

5.2. Comparison of groundwater discharge estimates

The results of groundwater discharge estimates obtained from seepage meter measurements, detailed differential streamflow gauging, differential streamflow gauging over time, and hydrograph separation are summarized in Table 3. It is seen that estimates from point-scale measurements range from 12 ± 15 to 41 ± 16 cm/d and are lower than inflows estimated using the other methods. Estimates obtained using catchment-scale methods (hydrograph separation) yield the highest inflow estimates ranging from 194 ± 31 to 289 ± 102 cm/d. For the shorter reaches 1 to 4, the estimates from detailed differential streamflow gauging range from 18 ± 46 to 333 ± 110 cm/d. These results suggest that groundwater discharge estimates depend on the spatial scale of the investigation method.

On 15 April 2015 for reaches 1 to 4, the groundwater contribution to streamflow estimated using seepage meter measurements accounted for 53%, 44%, 10% and 31%, respectively, of the net groundwater discharges estimated using the detailed differential streamflow gauging. This suggests that point-scale measurements are likely to underestimate

Table 3
Results of groundwater discharge estimates on 15 April 2015 and 6 August 2015, respectively.

Reach	Seepage meter measurements ± 2 SD, cm/d		Detailed differential streamflow gauging ± 2 SD_{Qgw}, cm/d				Differential streamflow gauging over time ± 2 SD_{Qdiff}, cm/d		Hydrograph separation ± 2 SD_{QBdiff}, cm/d	
	Apr	Aug	Apr	Aug	Apr	Aug	Apr	Aug	Apr	Aug
1	15 ± 6	–	28 ± 67	18 ± 46	–	–	–	–	–	–
2	12 ± 15	17 ± 7	27 ± 132	18 ± 94	159 ± 49	90 ± 29	161 ± 96	108 ± 54	289 ± 102	194 ± 31
3	32 ± 22	40 ± 38	333 ± 110	183 ± 73						
4	41 ± 16	–	135 ± 315	83 ± 183						

volumetric change in flow along the stream because they typically are taken on the sediment-water interface and therefore neglect groundwater discharge through the banks or that there is too few measurements over the variable streambed sediments. The partitioning of groundwater discharge into streambed seepage and bank seepage is likely to be particularly important in lowland alluvial catchments. Langhoff et al. (2006), for example, estimated the groundwater contribution to streamflow using differential streamflow gauging and compared it to explicit measurements of streambed seepage, bank seepage and overland flow. At one site they found that streambed seepage accounted for 38%, bank seepage for 25% and overland flow for 10%. At another site the numbers were 8%, 0% and 109%, respectively. Langhoff et al. (2006) measured streambed seepage at additional seven sites where it accounted for from a few percent to about 100% of the increase in streamflow. In the present paper, it could have been useful to also measure the groundwater discharge through the banks using an alternative seepage meter as done by Langhoff et al. (2006). However, this was not done because it is difficult and laborious to install such a seepage meter.

Moreover, on 6 August 2015 for reaches 2 and 3, the groundwater discharge estimates obtained using seepage meter measurements were 94% and 22%, respectively, of the estimates obtained using differential streamflow gauging. Thus, the discrepancy between seepage meter measurements and differential streamflow gauging is significantly larger in April than in August (Table 3). This is likely because bank seepage is more important when the groundwater system is “wet” with high water levels, high soil water content and partially-filled shallow runoff reservoirs (as in April) instead of “dry” (as in August).

Furthermore, the discrepancy between the groundwater discharge estimates obtained using seepage meter measurements and differential streamflow gauging is significant for the two groundwater dominated reaches, while it is insignificant for the two tile drainage dominated reaches. This is as expected because the groundwater dominated reaches of Knivsbaek stream are tightly connected with the aquifer through a wide riparian zone.

On 15 April 2015 and 6 August 2015 for the stream reach between S11 and S12, the groundwater contribution to streamflow estimated using hydrograph separation was approximately twice the net discharges estimated using the detailed differential streamflow gauging (Table 3). Results of Gonzales et al. (2009) suggest that simple filtering methods for hydrograph separation, including the UKIH method used in this paper, give lower groundwater discharge estimates than other non-tracer based methods and tracer-based methods. Thus, had we used other hydrograph separation methods than the UKIH method this would likely have increased the overestimation of groundwater discharge from baseflow separation.

We attribute the discrepancy between groundwater discharge estimates obtained using detailed differential streamflow gauging and hydrograph separation to the (in this case) erroneous assumption that the entire baseflow component of the streamflow hydrograph represents groundwater discharge to the stream (e.g. Halford and Mayer, 2000). Thus, other runoff components than groundwater discharge is likely to contribute to the long-term fluctuating component of the streamflow hydrograph; our findings from Knivsbaek catchment suggest that the most important other component is tile drainage discharge. To this end, we used a method (differential streamflow gauging over time) to exclude the tile drainage component from the streamflow hydrograph, and thereby extract a more reliable estimate of groundwater discharge to the stream. Thus, we found that the discrepancy between groundwater discharge estimates obtained using detailed differential streamflow gauging and differential streamflow gauging over time was insignificant (1% and 20% for April 2015 and August 2015, respectively).

Overall, for the studied stream, differential streamflow gauging provides a more reliable groundwater discharge estimate than that provided by seepage meter measurements. This is because differential streamflow gauging estimates the combined flux through the streambed and the banks while a seepage meter only measures the flux through the streambed. In addition, differential streamflow gauging also provides a more reliable groundwater discharge estimate than hydrograph separation. This is the result of the importance of tile drainage discharge for baseflow which cannot be recognised by pure non-tracer based hydrograph separation. Thus, our recommendation for future groundwater discharge estimation in lowland alluvial streams such as Knivsbaek is to use differential streamflow gauging. However, for hydrological systems in which hyporheic exchange is important, differential streamflow gauging does not capture this process which will limit the utility of the method. In addition, the more detailed (i.e. the shorter the reach) the larger the propagated uncertainty is relative to the estimated flux. This constrains the spatial resolution that can be obtained using this method. Overall, the use of more than one investigation method at point-, reach-, or catchment-scale will help to obtain a reliable estimate of the groundwater discharge component.

6. Conclusions

As part of research conducted at one of the HOBE project sites, field work was undertaken in the period Nov-2014 to Oct-2016 to demonstrate how combined use of methods at point-, reach-, and catchment-scale can be used to characterise groundwater discharge along a lowland alluvial stream. To this end, we compared and discussed groundwater discharge estimates obtained from these various methods.

The specific stream discharge was higher for the catchment outlet than for the gauging station at the upper third of the catchment, and it varied seasonally from less than $5\,\mathrm{l\,s^{-1}\,km^{-2}}$ during summer months and up to $> 60\,\mathrm{l\,s^{-1}\,km^{-2}}$ during winter events. The increase in streamflow was mainly due to tile drainage discharge in the upper reaches ($> 80\%$), while groundwater discharge was most important in the lower reaches ($> 60\%$). This spatial variation was controlled by topography, geology, regional groundwater flow pattern, and anthropogenic tile drainage.

Groundwater discharge estimates obtained using seepage meters at the lower reaches were about the double of those at the upper reaches, while the difference between measurements taken in April and those taken in August was insignificant. However, these estimates had large 95% confidence intervals, even though the streambed deposits appear to be homogeneous.

The groundwater discharge estimates obtained using detailed differential streamflow gauging were an order of magnitude larger than the estimates obtained using seepage meters. This is attributed to the partitioning of groundwater discharge into streambed seepage and bank seepage or that too few seepage meter measurements were taken to fully account for the spatial variability of streambed seepage. Furthermore, the estimates obtained using detailed differential streamflow gauging were half of those obtained using hydrograph separation, which was attributed to errors associated with the assumption that baseflow represents groundwater discharge to the stream. To this end, we used a method, which is referred to as differential streamflow gauging over time, to extract the tile drainage discharge from the streamflow hydrograph; a more reliable groundwater discharge estimate was thereby obtained. Moreover, we developed a novel method to calculate the uncertainty on groundwater discharge estimates obtained using hydrograph separation.

The overall conclusion is that the relative importance of different flow paths for discharging groundwater to a lowland alluvial stream varied between short reaches (0.5–1.5 km), and between April and August. These findings support the idea that groundwater and surface water interaction, even in lowland alluvial catchments, is spatially and temporally variable. Furthermore, the groundwater discharge estimates were dependent on the spatial scale of the investigation method. Thus, the use of more than one method at a site will help to obtain a reliable estimate of groundwater discharge from the other discharge components to the stream such as tile drainage discharge.

Acknowledgements

The manuscript was improved by review from Donald Rosenberry and three anonymous reviewers. This research has been carried out under the HOBE (Center for Hydrology) project, founded by the Villum Foundation. The detailed differential streamflow gauging were funded by the Food, Agriculture and Biotechnology, the Green Development and Demonstration Programme (GUDP). We would like to thank Lars Rasmussen, Jing Xie, Sofie Laursen, Peter Bo Callesen, and Tore Grønne for assistance in the field.

References

Anderson, M.P., 2005. Heat as a ground water tracer. Ground Water 43, 951–968. https://doi.org/10.1111/j.1745-6584.2005.00052.x.

Becker, M.W., Georgian, T., Ambrose, H., Siniscalchi, J., Fredrick, K., 2004. Estimating flow and flux of ground water discharge using water temperature and velocity. J. Hydrol. 296, 221–233. https://doi.org/10.1016/j.jhydrol.2004.03.025.

Cey, E.E., Rudolph, D.L., Parkin, G.W., Aravena, R., 1998. Quantifying groundwater discharge to a small perennial stream in southern Ontario. Canada. J. Hydrol. 210, 21–37. https://doi.org/10.1016/S0022-1694(98)00172-3.

Constantz, J., 2008. Heat as a tracer to determine streambed water exchanges. Water Resour. Res. 44, 1–20. https://doi.org/10.1029/2008WR006996.

Cranswick, R.H., Cook, P.G., 2015. Scales and magnitude of hyporheic, river-aquifer and bank storage exchange fluxes. Hydrol. Process. 3084–3097. https://doi.org/10.1002/hyp.10421.

Dahl, M., Nilsson, B., Langhoff, J.H., Refsgaard, J.C., 2007. Review of classification systems and new multi-scale typology of groundwater-surface water interaction. J. Hydrol. 344, 1–16. https://doi.org/10.1016/j.jhydrol.2007.06.027.

Eckhardt, K., 2005. How to construct recursive digital filters for baseflow separation. Hydrol. Process. 19, 507–515. https://doi.org/10.1002/hyp.5675.

Erickson, D.R., 1981. A study of littoral groundwater seepage at Williams Lake, Minnesota using separate meters and wells. University of Minnesota.

Frederiksen, R.R., Christiansen, A.V., Christensen, S., Rasmussen, K.R., 2017. A direct comparison of EMI data and borehole data on a 1000 ha data set. Geoderma 303, 188–195. https://doi.org/10.1016/j.geoderma.2017.04.028.

Gonzales, A.L., Nonner, J., Heijkers, J., Uhlenbrook, S., 2009. Comparison of different base flow separation methods in a lowland catchment. Hydrol. Earth Syst. Sci. 13, 2055–2068. https://doi.org/10.5194/hess-13-2055-2009.

Goodman, L.A., 1960. On the Exact Variance of Products. J. Am. Stat. Assoc. 55, 708–713.

Gustard, A., Bullock, A., Dixon, J.M., 1992. Low flow estimation in the United Kingdom. Institute of Hydrology.

Halford, K.J., Mayer, G.C., 2000. Problems associated with estimating ground water discharge and recharge from stream-discharge records. Ground Water 38, 331–342.

Hall, F.R., 1968. Base-flow recessions—a review. Water Resour. Res. 4, 973–983.

Hannula, S.R., Esposito, K.J., Chermak, J.A., Runnells, D.D., Keith, D.C., Hall, L.E., 2003. Estimating ground water discharge by hydrograph separation. Ground Water. https://doi.org/10.1111/j.1745-6584.2003.tb02606.x.

Harte, P.T., Kiah, R.G., 2009. Measured river leakages using conventional streamflow techniques: the case of Souhegan River, New Hampshire, USA. Hydrogeol. J. 17, 409–424. https://doi.org/10.1007/s10040-008-0359-1.

Hatch, C.E., Fisher, A.T., Revenaugh, J.S., Constantz, J., Ruehl, C., 2006. Quantifying surface water-groundwater interactions using time series analysis of streambed thermal records: method development. Water Resour. Res. 42, 1–14. https://doi.org/10.1029/2005WR004787.

Herschy, R.W., others, 1999. Hydrometry: principles and practices.

Jensen, K.H., Illangasekare, T.H., 2011. HOBE: a hydrological observatory. Vadose Zo. J. 10, 1–7. https://doi.org/10.2136/vzj2011.0006.

Johansen, O.M., Pedersen, M.L., Jensen, J.B., 2011. Effect of groundwater abstraction on fen ecosystems. J. Hydrol. 402, 357–366. https://doi.org/10.1016/j.jhydrol.2011.03.031.

Kalbus, E., Reinstorf, F., Schirmer, M., 2006. Measuring methods for groundwater, surface water and their interactions: a review. Hydrol. Earth Syst. Sci. Discuss. 3, 1809–1850. https://doi.org/10.5194/hessd-3-1809-2006.

Kliner, K., Knezek, M., 1974. The underground runoff separation method making use of the observation of groundwater table. Hydrol. hydromech. 22, 457–466.

Kronvang, B., Jeppesen, E., Conley, D.J., Søndergaard, M., Larsen, S.E., Ovesen, N.B., Carstensen, J., 2005. Nutrient pressures and ecological responses to nutrient loading reductions in Danish streams, lakes and coastal waters. J. Hydrol. 304, 274–288.

Langhoff, J.H., Rasmussen, K.R., Christensen, S., 2006. Quantification and regionalization of groundwater-surface water interaction along an alluvial stream. J. Hydrol. 320, 342–358. https://doi.org/10.1016/j.jhydrol.2005.07.040.

Lee, D.R., 1977. A device for measuring seepage flux in lakes and estuaries. Limnol. Oceanogr. 22, 140–147. https://doi.org/10.4319/lo.1977.22.1.0140.

Lowry, C.S., Walker, J.F., Hunt, R.J., Anderson, M.P., 2007. Identifying spatial variability of groundwater discharge in a wetland stream using a distributed temperature sensor. Water Resour. Res. 43, 1–9. https://doi.org/10.1029/2007WR006145.

McCallum, A.M., Andersen, M.S., Rau, G.C., Larsen, J.R., Acworth, R.I., 2014. River-aquifer interactions in a semiarid environment investigated using point and reach measurements. Water Resour. Res. 2815–2829. https://doi.org/10.1002/2012WR012922.Received.

Nyholm, T., Christensen, S., Rasmussen, K.R., 2002. Flow depletion in a small stream caused by ground water abstraction from wells. Ground Water 40, 425–437.

Opsahl, S.P., Chapal, S.E., Hicks, D.W., Wheeler, C.K., 2007. Evaluation of ground-water and surface-water exchanges using streamflow difference analyses. J. Am. Water Resour. Assoc. 43, 1132–1141. https://doi.org/10.1111/j.1752-1688.2007.00093.x.

Ovesen, N.B., 2011. Vandføringsmåling med vingeinstrument.

Ovesen, N.B., Iversen, H.L., Larsen, S.E., Müller-Wohlfeil, D.-I., Svendsen, L.M., Blicher, A.S., Jensen, P.M., 2000. Afstrømningsforhold i danske vandløb. Faglig rapport fra DMU nr 340.

Rasmussen, E.S., Dybkjær, K., Piasecki, S., 2010. Lithostratigraphy of the Upper Oligocene – Miocene succession of Denmark. Geol. Surv. Denmark Greenl. Bull. 22, 92.

Rosenberry, D.O., 2008. A seepage meter designed for use in flowing water. J. Hydrol. 359, 118–130. https://doi.org/10.1016/j.jhydrol.2008.06.029.

Rosenberry, D.O., 2005. Integrating seepage heterogeneity with the use of ganged seepage meters. Limnol. Oceanogr. Methods 3, 131–142. https://doi.org/10.4319/lom.2005.3.131.

Rosenberry, D.O., Briggs, M.A., Delin, G., Hare, D.K., 2016. Combined use of thermal methods and seepage meters to efficiently locate, quantify, and monitor focused groundwater discharge to a sand-bed stream. Water Resour. Res. 1–18. https://doi.org/10.1002/2016WR018808.Received.

Rosenberry, D.O., Pitlick, J., 2009. Local-scale variability of seepage and hydraulic conductivity in a shallow gravel-bed river. Hydrol. Process. 23, 3306–3318. https://doi.org/10.1002/hyp.7433.

Schmadel, N.M., Neilson, B.T., Stevens, D.K., 2010. Approaches to estimate uncertainty in longitudinal channel water balances. J. Hydrol. 394, 357–369. https://doi.org/10.1016/j.jhydrol.2010.09.011.

Sebok, E., Refsgaard, J.J., Stisen, S., Jensen, K.H., 2016. Using expert elicitation to quantify catchment water balances and their uncertainties. Water Resour. Res. 52, 5111–5131. https://doi.org/10.1002/2014WR015716.

Sellinger, C.E., 1996. Computer program for performing hydrograph separation using the rating curve method.

Sutton, J.E., Screaton, E.J., Martin, J.B., 2014. Insights on surface-water/groundwater exchange in the upper Floridan aquifer, north-central Florida (USA), from streamflow data and numerical modeling. Hydrogeol. J. 23, 305–317. https://doi.org/10.1007/s10040-014-1213-2.

Tallaksen, L.M., 1995. A review of baseflow recession analysis. J. Hydrol. 165, 349–370.

van Roosmalen, L., Christensen, B.S.B., Sonnenborg, T.O., 2007. Regional differences in climate change impacts on groundwater and stream discharge in Denmark. Vadose Zo. J. 6, 554. https://doi.org/10.2136/vzj2006.0093.

Xie, Y., Cook, P.G., Shanafield, M., Simmons, C.T., Zheng, C., 2016. Uncertainty of natural tracer methods for quantifying river-aquifer interaction in a large river. J. Hydrol. 535, 135–147. https://doi.org/10.1016/j.jhydrol.2016.01.071.